Published in final edited form as:

Oncogene. 2016 October 20; 35(42): 5552–5564. doi:10.1038/onc.2016.96.

WIP1 modulates responsiveness to *Sonic Hedgehog* signaling in neuronal precursor cells and medulloblastoma

Jing Wen[1], **Juhyun Lee**[1], **Anshu Malhotra**[1], **Rita Nahta**[3,4], **Amanda R. Arnold**[1], **Meghan C. Buss**[1], **Briana D. Brown**[1], **Caroline Maier**[1], **Anna M. Kenney**[1,3], **Marc Remke**[5], **Vijay Ramaswamy**[5], **Michael D. Taylor**[5], and **Robert C. Castellino**[1,2,3]

[1]Department of Pediatrics, Aflac Cancer and Blood Disorders Center, Atlanta, GA 30322, USA

[2]Children's Healthcare of Atlanta, Atlanta, GA 30322, USA

[3]Winship Cancer Institute, Emory University School of Medicine, Atlanta, GA 30322, USA

[4]Department of Pharmacology, Atlanta, GA 30322, USA

[5]Division of Neurosurgery, Arthur and Sonia Labatt Brain Tumour Research Center, and Program in Developmental and Stem Cell Biology, The Hospital for Sick Children, University of Toronto, Toronto, Ontario, Canada

Abstract

High-level amplification of the protein phosphatase *PPM1D* (*WIP1*) is present in a subset of medulloblastomas (MBs) that have an expression profile consistent with active *Sonic Hedgehog* (*SHH*) signaling. We found that *WIP1* overexpression increased expression of *Shh* target genes and cell proliferation in response to Shh stimulation in NIH3T3 and cerebellar granule neuron precursor (cGNP) cells in a p53-independent manner. Thus, we developed a mouse in which *WIP1* is expressed in the developing brain under control of the *Neurod2* promoter (*ND2:WIP1*). The external granule layer in early post-natal *ND2:WIP1* mice exhibited increased proliferation and expression of *Shh* downstream targets. MB incidence increased and survival decreased when *ND2:WIP1* mice were crossed with a *Shh*-activated MB mouse model. Conversely, *Wip1* knock out significantly suppressed MB formation in two independent mouse models of *Shh*-activated MB. Furthermore, *Wip1* knock-down or treatment with a WIP1 inhibitor suppressed the effects of Shh stimulation and potentiated the growth inhibitory effects of *SHH* pathway-inhibiting drugs in *Shh*-activated MB cells *in vitro*. This suggests an important cross-talk between *SHH* and *WIP1* pathways that accelerates tumorigenesis and supports WIP1 inhibition as a potential treatment strategy for MB.

Corresponding Author: Robert C. Castellino (rccaste@emory.edu), 1760 Haygood Dr., N.E., Room E394, Atlanta, GA 30322. Telephone: (404) 727-2078; Fax: (404) 727-4455.

Conflict of Interest

Drs. Castellino's, Kenney's, and Taylor's work has been funded by the NIH. Remaining authors declare no conflicts of interest.

Supplementary Information accompanies the paper on the *Oncogene* website (http://www.nature.com/onc).

Keywords

WIP1; PPM1D; Hedgehog; p53; medulloblastoma

Introduction

Medulloblastoma (MB) is the most common malignant brain tumor of childhood. Unfortunately, current therapeutic regimens are associated with numerous long-term side effects.[1] And, despite clinical advances, up to 30% of children with MB experience tumor progression or recurrence, for which no cure exists.[2] Continued advances in therapy demand a better understanding of the molecular drivers of MB and treatment responsiveness.

Recent studies suggest that MB can be divided into at least four sub-groups based on gene expression and methylation profile: *Wingless* (*WNT*), *Sonic Hedgehog* (*SHH*), Group 3, and Group 4.[3] One-quarter of MBs bear a signature of active *SHH* signaling. Clinically viable small molecule inhibitors of SHH signaling have been developed, and Phase I/II clinical trials have demonstrated efficacy of SHH-inhibiting drugs against *SHH* MBs.[4] Unfortunately, resistance to SHH inhibitors develops quickly, and mechanisms of resistance are not fully understood.

Cytogenetics have previously shown that one-third of MBs exhibit gain of the long arm of chromosome 17 (17q) or isochromosome 17q (i17q), which is associated with poor disease-related survival.[5] Surprisingly, the tumor suppressor gene, *TP53*, on chromosome 17p13, is usually wild-type in most MBs that exhibit loss of heterozygosity of 17p.[6] Mutations of *TP53* are constrained almost exclusively to *WNT* and *SHH* MBs and confer a dismal prognosis for survival in patients with *SHH* MBs. However, *TP53* mutations are present in less than 10% of MBs.[7] Yet, p53 function is compromised in a larger percentage of tumors, especially in aggressive histologic subtypes of MB.[8] Northcott *et al*. have shown that a subset of MBs that have a signature of *SHH* pathway activation have high-level amplification of the chromosomal locus of *WIP1* (*wild-type p53-induced phosphatase 1*; *protein phosphatase, magnesium-dependent 1, delta, PPM1D*) on chromosome 17q22-q23.[9]

We found that *WIP1* overexpression in NIH/3T3 and cerebellar granule neuron precursor (cGNP) cells, a well-characterized MB cell of origin,[10–13] increased expression of *Shh* target genes and cell proliferation in response to Shh stimulation in a p53-independent manner. *WIP1* transgenic mice showed evidence of increased proliferation and expression of *Shh* downstream target genes in the external granule layer, where cGNPs arise and proliferate during early post-natal cerebellar development. When *WIP1* transgenic mice were crossed with *Shh*-activated, *SmoA1/SmoA1* MB-prone mice, MB incidence increased and MB-associated survival decreased. Conversely, *Wip1* knock out significantly suppressed MB formation in *SmoA1/SmoA1* and tamoxifen-induced *Math1*-cre^{ER}; *Ptc1 fl/fl* mice. shRNA-mediated knock-down of *Wip1* or treatment with a WIP1 inhibitor blocked the effects of Shh stimulation and potentiated the growth inhibitory effects of the *SHH* pathway-inhibiting drugs in *SmoA1*/*SmoA1* or *Math1*-creER+; *Ptc1* fl/fl MB cells under cell culture conditions. This suggests an important cross-talk between *SHH* and *WIP1* signaling that accelerates MB tumorigenesis and that may be targetable with small molecules that inhibit WIP1 function.

Results

WIP1 promotes cell growth through sonic hedgehog signaling pathways

Previous studies support cross-talk between WIP1 and the *SHH* signaling pathway in multiple types of cancer, including MB.[14, 15] To better understand this, we used NIH/3T3 cells stably transfected with a GLI-responsive Firefly luciferase reporter and a constitutive Renilla-luciferase expression vector (shh-LIGHT2) or with a Gli-dependent enhanced green fluorescent protein (EGFP) reporter (shh-EGFP), which provide downstream read-outs for activation of *SHH* signaling.[16, 17] Immunofluorescence (IF) detected increased GFP in yellow fluorescent protein (YFP)-*WIP1* (YFP-*WIP1;* LentiORF-YFP-*WIP1*)-transduced shh-EGFP cells, following stimulation with recombinant Shh (Shh) (Fig. 1A). We also found increased expression of Firefly luciferase in Shh-stimulated, YFP-*WIP1*-transduced shh-LIGHT2 cells, relative to controls (Fig. 1B). Quantitative real-time, RT-PCR (qRT-RT-PCR) confirmed increased expression of the downstream target of *Shh* signaling, *Gli1*, following Shh stimulation (Fig. 1C). Flow cytometry revealed a significant increase in the percentage of YFP-*WIP1*-transduced shh-EGFP cells in S phase following Shh stimulation (Fig. 1D). Overall, this shows that WIP1 increases proliferation through Shh-dependent and –independent mechanisms.

WIP1 promotes hedgehog signaling through *p53*-independent pathways

Although earlier studies have shown that *WIP1* promotes growth primarily through p53 signaling pathways, recent publications suggest that the interaction between WIP1 and *SHH* signaling occurs independent of p53.[15] To validate this prior finding, we transduced shh-EGFP cells with either *Trp53* shRNA or YFP-*WIP1*. In contrast to the prior report in which *TP53* knockdown enhanced Shh signaling, in shh-EGFP cells, knock-down of *Trp53* did not affect Shh-stimulated expression of *Gli1* in the presence or absence of *WIP1* (Fig. 2A, Fig. S1).

Next, we treated shh-EGFP cells with Nutlin-3a, the active enantiomer of Nutlin-3, which disrupts the interaction between p53 and Mdm2, preventing proteasome-mediated p53 degradation.[18] Nutlin-3a and p53 shRNA alter p53 activity in opposite ways. sh*Trp53* reduces p53 activity by blocking p53 expression, while Nutlin-3a activates p53, by stabilizing the p53 protein. Treatment with Nutlin-3a suppressed activation of the *Gli* promoter in shh-EGFP cells, as evident by suppression of GFP as well as of expression of the proliferation marker Ki-67 in Shh-stimulated, empty vector-transduced shh-EGFP cells. Nutlin-3a treatment of YFP-*WIP1*-transduced shh-EGFP cells similarly suppressed activation of the *Gli* promoter and Ki-67 following Shh stimulation (Fig. 2B–C). And, Nutlin-3a suppressed Shh-stimulated expression of *Gli* in shh-EGFP cells transduced with empty vector or YFP-*WIP1* (Fig. 2D). This suggests that high p53 levels override growth support from Shh or transduced *WIP1*.

WIP1 enhances *Shh* signaling in cerebellar GNPs

To understand the significance of high expression or amplification of *WIP1* in MB tumorigenesis, we transduced cGNPs from post-natal day seven (P7) wild-type mice with

empty vector or YFP-*WIP1*. This resulted in increased expression of the downstream *Shh* target genes *Gli1* and *Ptc1* (Fig. 3B).

To determine dependence on p53 signaling, we transduced wild-type P5 cGNPs shNC or sh*Trp53* in combination with empty vector or YFP-*WIP1* (Fig. 3A, D). *WIP1* overexpression enhanced proliferation, while stimulation with Shh inhibited apoptosis. Furthermore, knock-down of *Trp53* did not significantly affect Shh-stimulated proliferation in the presence or absence of overexpressed *WIP1* (Fig. 3A, C). This also suggests that *WIP1* augments *Gli1* through *p53*-independent pathways. Nutlin-3a significantly suppressed Shh-stimulated proliferation of cGNPs transduced with empty vector or YFP-*WIP1*, which again suggests that high levels of p53 override growth support provided by Shh or transduced *WIP1* (Fig. 3E).

WIP1 enhances *Shh* signaling and proliferation in the neonatal cerebellum

To understand the role of *WIP1* in MB tumorigenesis, we developed a mouse in which human *WIP1* is expressed under the control of the *Neurod2* promoter (*ND2:WIP1*), which has previously been used to drive constitutive expression of activated Smoothened in the developing cerebellum (Fig. 4A).[19] Embryos were screened for *ND2:WIP1* transgene expression by conventional PCR (Fig. 4B). *WIP1* expression was significantly higher in the P7 cerebellum of *ND2:WIP1* transgenic mice, compared to age-matched, wild-type controls (Fig. 4C). *ND2:WIP1* transgenic founder #12 was used in subsequent experiments since *WIP1* expression was highest in the cerebellum of these mice by qRT-RT-PCR.

ND2:WIP1 transgenic mice are viable and do not exhibit any morphologic abnormalities, other than fewer cerebellar lobules at P5, versus controls (Fig. 4D). Immunohistochemistry (IHC) for Ki-67 demonstrated increased proliferation in the external granule layer (EGL) of the P5 cerebellum of *ND2:WIP1* and *SmoA1*/*SmoA1* mice, compared to controls. IHC for *Shh* downstream targets also showed increased expression of Cyclin D1 (Ccnd1) in the P5 EGL of *ND2:WIP1* and *SmoA1*/*SmoA1* mice (Fig. 4E). Consistent with published findings, which showed that aberrant *Shh* signaling in the P7 cerebellum of *SmoA1* mice leads to $p27^{Kip1}$ (p27) mis-localization and increased cGNP proliferation throughout the EGL,[20] double labeling with Ki-67 and p27 showed that, at P5, the Ki-67+ EGL in *ND2:WIP1* and *SmoA1*/*SmoA1* mice is thicker than wild-type mice. Conversely, the p27+ cell layer at the base of the EGL is thicker in wild-type, compared to *ND2:WIP1* and *SmoA1*/*SmoA1* mice (Fig. 4F). Thus, mis-localization of p27 in the developing cerebellum of *ND2:WIP1* transgenic mice may alter cell cycle progression and promote MB formation.

WIP1 promotes MB tumorigenesis in a hedgehog-activated model

Previously published reports suggest that increased *WIP1* expression alone does not promote formation of *de novo* tumors.[14, 21] Similarly, we did not detect *de novo* MBs in *ND2:WIP1* mice. However, when we mated *ND2:WIP1* mice with *SmoA1*/*SmoA1* mice, the incidence of MBs increased, mice presented with MB symptoms at a younger age, and *SmoA1*/*SmoA1*; *ND2:WIP1*+ mice exhibited reduced overall MB-related survival (Fig. 5A–B). Western blotting showed increased expression of Mdm2 and reduced expression of Trp53 in MBs derived from *SmoA1*/*SmoA1*; *ND2:WIP1*+ mice (Fig. 5C). And, MB cells from

symptomatic *SmoA1*/*SmoA1*; *ND2:WIP1*+ mice exhibited increased viability compared to MB cells derived from symptomatic *SmoA1*/*SmoA1*; *ND2:WIP1*-mice (Fig. 5D). In human *SHH*-activated MBs with focal *WIP1* amplification, we validated increased *WIP1* expression (Fig. 5G).

Wip1 knock-out suppresses MB formation

Studies published to date show that *Wip1* knock-out of impairs spermatogenesis. However, *Wip1*−/− mice are viable and resistant to tumor formation.[22] No studies to date have described abnormalities in the developing nervous system of *Wip1*−/− mice. Using IHC, we found that the portion of the EGL in P5 *Wip1*−/− mice that stained positive for Ki-67 and the downstream marker of *Shh* pathway activation, Ccnd1, was thinner than in P5 *Wip1*+/+ mice (Fig. 6A). This suggests that the P5 EGL of *Wip1*−/− mice contains fewer proliferating, *Shh*-activated cells compared to the EGL of *Wip1*+/+ mice. Given this finding, and since other groups have shown that *Wip1* loss impairs tumor formation,[15, 23] we mated *Wip1*−/− mice with constitutive (*SmoA1*/*SmoA1*) or conditional (*Math1*-cre^{ER}; *Ptc1* fl/fl) mouse models of *Shh*-activated MB. In both models, *Wip1* knockout significantly suppressed *de novo* MB formation (Fig. 6B–C).

WIP1 inhibition suppresses hedgehog signaling and proliferation

To examine the effects of pharmacologic WIP1 inhibition, we treated shh-EGFP cells with the WIP1 small molecule inhibitor, CCT007093. Shh stimulation of shh-EGFP cells transduced with YFP-*WIP1* resulted in increased activation of the *Gli* promoter, with increased GFP, and increased Ki-67, relative to controls. Treatment of YFP-*WIP1*-transduced shh-EGFP cells with CCT007093 significantly inhibited both GFP and staining for Ki-67, following stimulation with Shh (Fig. 7A–B). Similarly, treatment of YFP-*WIP1*-transduced GNPs with CCT007093 significantly inhibited proliferation following Shh stimulation (Fig. 7C).

We also examined pharmacologic WIP1 inhibition in MB cells cultured from *SmoA1*/*SmoA1* or tamoxifen-induced, *Math1*-cre^{ER}+; *Ptc1* fl/fl mice. The small molecules SAG and SANT-1 stimulate or inhibit *Shh* signaling, respectively. SAG stimulated, while SANT-1 inhibited the growth of MB cells derived from *SmoA1*/*SmoA1*; *ND2:WIP1*+ mice in short-term cultures. Treatment of MB cells from a *SmoA1*/*SmoA1*; *ND2:WIP1*+ mouse with lentivirus that knocked down *Wip1* (not shown) or with CCT007093 inhibited the growth-promoting effects of SAG and potentiated the anti-proliferative effects of SANT-1 (Fig. 8A, left). Effects of WIP1 inhibition on cell viability correlated with reduced expression of the downstream *Shh* target *Gli1* in CCT007093-treated *SmoA1*/*SmoA1*; *ND2:WIP1*+ MB cells (Fig. 8A, right).

We also studied the effects of small molecules that inhibit Shh and WIP1 signaling alone and together in the *SmoA1*/*SmoA1*; *Wip1*+/+ and tamoxifen-induced *Math1*-cre^{ER}; *Ptc1* fl/fl MB models, which do not have high *Wip1* expression. Treatment of MB cells with CCT007093 alone resulted in a similar suppression of cell viability, compared to treatment with either Shh small molecule inhibitor: cyclopamine or the clinically-relevant drug LDE225[24] (Fig. 8B–C). Reduction in cell viability correlated with reduced expression of

Gli1 and *Ptc1* (Fig. 8C, right-hand panels). Combined treatment with CCT007093 and a Shh-inhibiting drug resulted in a further reduction in MB cell viability, although this did not appear to be associated with further reductions in expression of *Gli1* and *Ptc1*. We also employed BrdU incorporation and IF for Cleaved Caspase 3 to assay for proliferation and cell death, respectively, in MB cells isolated from symptomatic *SmoA1*/*SmoA1*+; *Wip1*+/+ mice. Cyclopamine and LDE225, as well as CCT007093, significantly inhibited MB cell proliferation, alone or in combination, under cell culture conditions. However, LDE225, alone or in combination with CCT007093, also significantly increased MB cell death (Fig. 8B, right-hand panels).

Discussion

WIP1 is a serine/threonine protein phosphatase that is important in the DNA damage response. Through its phosphatase activity on proteins crucial for cell cycle regulation or DNA damage response, including Atm, p53, Chk1, Chk2, Mdm2, Mdm4, p38MAPK, and γ-H2AX, WIP1 functions in a negative feedback control loop to maintain homeostasis following exposure to DNA-damaging agents.[25] However, gene amplification, high-level expression, or specific C-terminal mutations can result in WIP1 functioning as an oncoprotein.

On its own, *Wip1* overexpression does not promote spontaneous tumor formation. But, *Wip1* cooperates with validated oncogenes, including *c-myc*, *Erbb2*, *Ras*, and *E1A*, to transform mouse embryonic fibroblasts.[22, 26] Double transgenic mice that express both *Erbb2* and *Wip1* under control of the MMTV promoter exhibit a shorter onset to the development of breast tumors.[21] And, amplification of the chromosomal locus of *WIP1*, 17q22-q23, has been described in numerous human malignancies that are *wild-type* for *TP53*, including MB.[9, 26, 27]

By fluorescence *in situ* hybridization and comparative genomic hybridization we previously identified 64% of MBs with amplification of the *WIP1* locus.[28] We have described increased *WIP1* expression in non-*Wingless* (*WNT*) activated MBs,[29] a signature that is often associated with inferior patient survival.[30] And, we have shown that increased *WIP1* expression in MB is associated with poor overall and event-free survival. Recently, we have shown increased *WIP1* expression in Group 3&4 MBs, which have a high incidence of metastasis at diagnosis. And, we have described an important interaction between WIP1 and CXCR4 signaling that may promote MB metastasis.[31]

Following up on the work of Northcott *et al.* in which they showed that a subset of MBs that have a gene signature of active *SHH* signaling also have high-level amplification of the chromosomal locus of *WIP1*,[9] we found that *WIP1* overexpression in NIH/3T3 cells and cGNPs enhanced proliferation and expression of *Shh* target genes in response to Shh stimulation. Overall, our findings were in agreement with Pandolfi *et al.* in which they show that *WIP1* increased the transcriptional activity of *GLI1* in the colon cancer cell line HCT116.[15] Interestingly, neither wild-type nor phosphatase-deficient, mutant (*WIP1* D314A) *WIP1* activated a *GLI*-dependent promoter in HCT116 cells. But, in patient-derived SSM2c melanoma and MCF7 breast cancer cells, which express high levels of *WIP1* at

baseline, transfection with exogenous *WIP1* increased activation of a *GLI*-dependent promoter and *GLI1* mRNA expression. This suggests that cross-talk between *WIP1*and *SHH* signaling may be modulated by tumor or cell line-specific factors that are still unknown.

Investigators have previously shown that WIP1 inactivates p53[32] and that p53 and GLI1 function in a negative feedback loop.[33] We investigated whether the interaction between *WIP1* and *SHH* signaling in MB is p53-dependent. Using expression plasmids that contain a luciferase reporter, investigators have shown that p53 negatively regulates the activity, localization, and expression of GLI1.[34] We found that *WIP1* overexpression enhanced proliferation, while stimulation with Shh inhibited apoptosis. Furthermore, knock-down of *Trp53* did not significantly affect Shh-stimulated proliferation in the presence or absence of overexpressed *WIP1*. This suggests that *WIP1* augments *Gli1* expression through p53-independent pathways. That Nutlin-3a significantly suppressed Shh-stimulated proliferation of cerebellar GNPs transduced with empty vector or YFP-*WIP1*, suggests that, in cGNPs, the effects of high levels of p53 override whatever growth support is provided by Shh or transduction with *WIP1* lentivirus.

To further understand *WIP1* mechanisms *in vivo*, we developed a mouse in which *WIP1* is expressed under control of the *Neurod2* promoter (*ND2:WIP1*). Compared to wild-type controls, the EGL of P5 *ND2:WIP1* mice exhibited increased proliferation and expression of the *Shh* downstream target Ccnd1. Although a few >12-month-old *ND2:WIP1* mice exhibited lethargy or preferential turning in one direction, we were unable to find histologic evidence of MB in these mice. This is consistent with the findings of other groups who have been unable to promote tumor formation *in vivo* by overexpressing *WIP1* alone, but suggests that activation of growth promoting signaling pathways by *WIP1* may predispose cells in the early post-natal EGL of *ND2:WIP1* mice to malignant transformation in the presence of other oncogenes.[14, 21, 26]

Investigators have previously shown that co-injected of RCAS-*WIP1* and -*Shh* expression constructs into neonatal mice increased the incidence of MB.[35] And, knock-down of *PTCH1* accelerated the growth of flank xenografts of *WIP1* high-expressing patient-derived melanoma cells in athymic-nude mice.[15] We validated increased *WIP1* expression in *SHH*-activated MB tissues with focal amplification of the *WIP1* locus, compared to cerebellar controls and compared to MBs with balanced alterations in chromosome 17. And, when we mated *ND2:WIP1* transgenic with *SmoA1/SmoA1* mice, MB incidence increased and survival decreased. This confirmed an important interaction between *WIP1* and *SHH* signaling that promotes MB tumorigenesis.

Since other groups have shown that *Wip1* loss inhibits tumor formation[23] and that WIP1 is a viable target for cancer therapy,[15, 25, 36–38] we examined the effects of *Wip1* loss or inhibition in *Shh*-activated models of MB. *Wip1* knock out reduced the thickness of the proliferating Ki-67+ or Ccnd1+ P5 EGL. *Wip1* knock out also significantly suppressed MB formation in two independent *Shh*-activated mouse models of MB. Treatment with a lentivirus that knocks down *Wip1* or with the WIP1 inhibitor CCT007093 blocked the effects of Shh stimulation and potentiated the effects of the *SHH* pathway-inhibiting drugs SANT-1, cyclopamine, or the clinically-relevant SHH inhibitor, LDE225, on the growth of

either *SmoA1*/*SmoA1* or tamoxifen-induced *Math1*-creER+; *Ptc1* fl/fl MB cells *in vitro*. These findings suggest that WIP1 is an important, druggable molecular target for MB treatment.

Materials and Methods

Lentiviral Particle Production and Infection

RFP control and YFP-*WIP1* Precision LentiORF expression constructs (Thermo Scientific) were modified in the Custom Cloning Core Facility (CCCF). EGFP-negative control and sh*Trp53* short hairpin RNA lentiviral expression constructs have been previously described.[31] psPAX2 and pVSVG plasmids (gifts, Dr. H. Trent Spencer, Emory University). pLKO.1 (gift, Dr. Rita Nahta, Emory University). Production and transduction with lentiviral particles were previously described.[29]

Cell Culture

shh-EGFP and shh-LIGHT2 cells (gifts, James Chen, Stanford University) have been described previously.[16] Cells were maintained in DMEM medium with high glucose, 1x PenStrep (100 U/mL Penicillin and 100μg/mL Streptomycin), 10% (vol/vol) heat-inactivated FBS at 37°C in 5% CO_2 under selection with 400μg/mL Zeocin (Life Technologies). Cells were authenticated by STR profiling within the last 6 months and are screened for mycoplasma contamination every 6 months (MycoAlert Detection Kit; Lonza Group).

Cerebellar GNPs were generated, as described.[39] A Percoll gradient was used to purify re-suspended GNPs, as previously described.[13] Cells were plated onto poly-DL-ornithine-coated 24-well plates with glass coverslips for histology experiments or plated onto poly-DL-ornithine-coated 6-well plates for RT-PCR experiments. Shh (3μg/mL) was added to samples within the Shh treatment groups. Media containing serum was replaced with serum-free media with and without Shh after a 3 hour incubation period. At this time, 20μl of respective viruses were added to each well. Immunofluorescence or RT-PCR was performed on samples 48 and 72 hours post-treatment.

Proliferation Assays

1×10^5-2.5×10^5 shh-EGFP cells were plated on 6-well plates or 1×10^6 GNPs on poly-L-ornithine-coated 24-well plates in triplicate and under conditions of serum starvation. Twenty-four hours later, cells were transduced with RFP-tagged control or YFP-tagged *WIP1* lentivirus with or without control (pLKO.1) or sh*Trp53* lentivirus, and treated with vehicle or 3μg/mL Shh-N. Alternatively, cells transduced with control or YFP-tagged *WIP1* lentivirus were treated for 24 hours with vehicle, 8μM Nutlin-3a (Selleck, Houston, TX) , or 5μM CCT007093 (Selleck). After Shh-N stimulation and/or drug treatment, cells were harvested with 0.25% trypsin EDTA (Mediatech) and counted by trypan blue exclusion using a Cellometer Vision CBA (Nexcelom).

Luminescence

24-well tissue culture plates were coated with 1X Poly-L-Ornithine (Corning Inc., Lowell, MA, 25–055-CV). 2.5×10^5 Shh-LIGHT2 cells[17] were plated per well in 500μl media

containing DMEM with 10%FBS and 1% P/S. 24 hours later, cells were changed to DMEM with 0.5% FBS and transduced with red fluorescent protein (RFP)-tagged control (RFP-CTRL) or yellow fluorescent protein (YFP)-tagged *WIP1* (YFP-*WIP1*) lentivirus. 24 hours later, cells were stimulated with vehicle or Shh (3μg/mL) for 24 hours. Luciferase activity was assayed using the Dual Luciferase Reporter Assay System (Promega, Madison, WI, # E1910), according to manufacturer's instructions.

Cell Cycle Analysis

Forty-eight hours after transducing shh-EGFP cells with control or YFP-tagged *WIP1* lentivirus and stimulating with vehicle or 3μg/mL Shh-N, 10μM EdU was added to media and incubated for 5 hours. Cells were harvested by scraping, fixed, permeabilized, and incubated with Click-iT® EdU reagents, including FxCycle™ Violet, per the manufacturer's protocol (Life Technologies). Samples were analyzed using a BD FACS Canto II cytometer (BD Biosciences, San Jose, CA, USA) with BD FACS Diva software.

Quantitative Real-Time, RT-PCR

Total cellular RNA was extracted, as previously described.[29] qRT-RT-PCR reactions containing cDNA, Sybr Green PCR Master Mix (Life Technologies) and primers for *WIP1*, *Gli1, Ptc1, Trp53*, and/or *Glyceraldehyde-3 Phosphate Dehydrogenase* (*Gapdh*) were run on an ABI 7500 Real-Time PCR Cycler (Life Technologies) using absolute quantification with a standard curve. Primer sequences available upon request. Absolute gene expression was determined based on standard curves. Target gene expression was normalized to *Gapdh* expression.

Western Blotting

Protein was extracted, quantified, and probed with antibodies, as described.[40] Whole cell lysates were extracted using RIPA buffer (Cell Signaling). Antibodies used included p53 (Cell Signaling, Danvers, MA), Mdm2 (EMD Millipore, Billerica, MA), WIP1 (Bethyl, Montgomery, TX), and β-actin (Sigma-Aldrich, St. Louis, MO). Secondary antibodies Alexa Fluor 680 goat anti-mouse IgG (Life Technologies) or IRDye 800 goat anti-rabbit IgG (Rockland, Gilbertsville, PA) were used at a dilution of 1:5,000. Immunoblots were imaged as previously described.[29]

Tissue Handling and Immunohistochemistry

Mouse brains were sectioned sagittally down the midline and fixed in formalin. Tissue blocks were paraffin-embedded and cut into 5μm sections. Following antigen retrieval, tissues were blocked and incubated with α-Ki67 (1:500; Vector, VP-RMO4) or Ccnd1 (1:100; Thermo Scientific, SP4) overnight at 4°C, then incubated with biotinylated goat anti-rabbit IgG (1:300; Vector, BA-1000). Slides were stained with hematoxylin and mounted using VectaMount (Vector). Images were captured with an Olympus DP70 digital camera, and were analyzed using the DP Controller software package (Olympus). Images were processed for publication using Adobe Photoshop Elements 5.0 (Adobe Systems).

BrdU Labeling

BrdU (Fisher Scientific, # BP 2508250) was added to medium (3μg/ml) for 4 hrs, and fixed in 4% paraformaldehyde (PFA). Cells were incubated with α-BrdU (BD Biosciences, San Jose, CA, #347580) (1:1000), and then Alexa Fluor 594-conjuated Affinipure F (ab')2 fragment goat anti-mouse IgG (H+L) secondary antibody (Jackson ImmunoResearch, West Grove, PA, code:115–586-003). Coverslips were mounted with Vectashield with DAPI (Vector, Burlingame, CA, H-1500). Images were obtained from 10 representative areas on each coverslip using a Leica DM2500 microscope with a DFC 365FX digital camera and the Leica Application Suite-Advanced Fluorescence software package (Leica Microsystems).

Immunofluorescence Quantitation

Quantitation of BrdU or Cleaved Caspase 3 positive cells was preformed using CellProfiler.[41] Two analysis pipelines were used to identify nuclear labeling (DAPI or BrdU) or cytoplasm labeling (Cleaved Caspase 3) in .TIFF images: (1) Color to Gray module converted images to greyscale, and (2) Identify Primary Objects module was used to optimize program recognition of individual positive cells. Positive cells were identified based on diameter and fluorescence intensity. BrdU or Cleaved Caspase 3-positive counts were divided by DAPI-positive nuclei counts. Cell counting was single blinded: the experimenter was conscious of experimental details, but the unbiased observer, who counted the cells, was blinded from sample details.

Immunofluorescence

Coverslips were placed into 24-well plates, coated with poly-L-ornithine, and seeded with 5×10^4 shh-EGFP cells or 1×10^6 GNPs and treated as described for Proliferation. After 48 hours, cells were fixed with 4% PFA and blocked, then incubated with α-WIP1 (1:100; Bethyl, A300–664A) or Ki67 (1:500; Vector, VP-Rmo4) overnight at 4°C, then incubated with secondary antibody (1:500; Alexa Fluor® 594 goat anti-rabbit IgG, A-11012, Life Technologies). Coverslips were mounted on slides with Vectashield with DAP1 (Vector, H-1500). High-magnification images were obtained from 10 representative areas on each coverslip using a Leica DM2500 microscope with a DFC 365FX digital camera and Leica Application Suite-Advanced Fluorescence (Leica Microsystems).

P5 brains were sectioned sagittally down the midline, and fixed in 10% formalin. Following antigen retrieval, tissues were blocked, and incubated with α-Ki67 (SP6) (1:250 dilution, Abcam, ab16667) overnight at 4° C, followed by incubation with secondary antibody (Alexa Fluor 549 goat anti-rabbit IgG. Life Technologies, A11012). P27 (Kip1) (1:100 dilution, BD Transduction laboratories, 610241) was then added, followed by a second secondary antibody (Alexa Fluor 488 goat anti-mouse IgG. Life Technologies, A11029). Tissues were mounted on slides with Vectashield mounting medium with DAPI (Vector, H-1500), and imaged at 40X, as above.

Mice

Full-length *WIP1* was isolated from a Tre-tight *WIP1* expression plasmid (gift, Lawrence A. Donehower, Baylor College of Medicine, Houston, TX) by restriction digest using *Kpn*I-*Hind*III and ligated between *Xba*I-*Apa*I into a pcDNA3.1/V5-His B vector (gift, Dr. James

Olson, Fred Hutchinson Cancer Center, Seattle, WA) that already contained the *NeuroD2* promoter between *EcoR*I-*Xho*I. *WIP1* orientation was confirmed and sequenced. A fragment containing the *NeuroD2* promoter, *WIP1*, and a polyadenylic acid sequence was isolated by restriction digest (*Hind*III-*Avr*II, 4036 bp), purified using Qiagen columns, and provided to the Emory Transgenic Mouse & Gene Targeting Core for zygote (E0.5 fertilized eggs) injection. Transgene expression was quantified on genomic DNA derived from tail snips using reverse transcription-PCR (RT-PCR) with the following primers: TCCTGGGAAGTGATGGACTTTGGA (forward) and ACGATGGCACTTGTGTTATCTGCC (reverse).

SmoA1 transgenic mice, on a C57Bl/6 background (gift, James Olson, Fred Hutchinson Cancer Center, Seattle, WA), were mated for at least six generations and then test crossed with wild-type C57Bl/6 mice to ensure a genotype of *SmoA1*/*SmoA1*.[19] Similarly, *ND2:WIP1* transgenic mice were mated with *SmoA1*/*SmoA1* mice for at least six generations and then test crossed with wild-type C57Bl/6 mice to ensure the desired genotypes. Mice used for the MB study represent at least six generations, beginning with the F2 generation.

Wip1+/− mice (gift, Dr. Xiongbin Lu, MD Anderson Cancer Center, Houston, TX), on a 129Sv background, were bred to obtain desired genotypes.[42] *Wip1*+/− mice were mated with *SmoA1*/*SmoA1* mice for at least six generations and test crossed with wild-type C57Bl/6 mice to ensure desired genotypes. *Math1*-cre^{ER}; *Ptc1* fl/fl mice[43] were mated with *Wip1*+/− mice for at least six generations to obtain desired genotypes. All mice were maintained on a mixed C57Bl/6 × 129Sv background. Mice were administered 1mg tamoxifen by gavage on P7. All mice used for MB studies represent at least six generations, beginning with the F2 generation.

All mice were housed in an AALAC–accredited facility and maintained in accordance with NIH guidelines. All animal care and experiments were approved by the Emory University IACUC (Protocol # DAR-2002073).

Statistical Analysis

Sample size was chosen based on a previous report.[44] Simple randomization was used in experiments where randomization was based on a single sequence of random assignments (control versus treated).[45] Mice bearing tumors were selected based on symptoms, described previously.[46] Gene expression in human MB samples has been described in the Vanner dataset;[47] copy number was determined using Affymetrix SNP 6.0[9]. The Vanner dataset was run on the Affymetrix 1.0T platform. All results were analyzed using a two-tailed Student's t-test or one-way ANOVA in Microsoft Excel or Graphpad Prism 4 software to assess statistical significance. Normality of data was determined by Chi-square testing and by reviewing graphical (i.e. boxplot) distribution of data. Values of $p < 0.05$ were considered statistically significant.

Supplementary Material

Refer to Web version on PubMed Central for supplementary material.

Acknowledgments

We acknowledge Drs. James Olson and Xiongbin Lu for providing mice and expression constructs, and Dr. Oskar Laur in the Emory University CCCF for plasmid construction. Work was supported by the NIH (1R01CA172392, R.C.C.; CA159859, M.D. Taylor), St. Baldrick's Foundation (R.C.C.), CURE Childhood Cancer Foundation (R.C.C.), and the Dr. Mildred-Scheel Foundation (M.R.).

References

1. von Hoff K, Hinkes B, Gerber NU, Deinlein F, Mittler U, Urban C, et al. Long-term outcome and clinical prognostic factors in children with medulloblastoma treated in the prospective randomised multicentre trial HIT'91. Eur J Cancer. 2009; 45:1209–1217. [PubMed: 19250820]
2. Torres CF, Rebsamen S, Silber JH, Sutton LN, Bilaniuk LT, Zimmerman RA, et al. Surveillance scanning of children with medulloblastoma. N Engl J Med. 1994; 330:892–895. [PubMed: 8114859]
3. Northcott PA, Korshunov A, Witt H, Hielscher T, Eberhart CG, Mack S, et al. Medulloblastoma comprises four distinct molecular variants. J Clin Oncol. 2011; 29:1408–1414. [PubMed: 20823417]
4. Samkari A, White J, Packer R. SHH inhibitors for the treatment of medulloblastoma. Expert Rev Neurother. 2015:1–8.
5. Ellison D. Classifying the medulloblastoma: insights from morphology and molecular genetics. Neuropathol Appl Neurobiol. 2002; 28:257–282. [PubMed: 12175339]
6. Burnett ME, White EC, Sih S, von Haken MS, Cogen PH. Chromosome arm 17p deletion analysis reveals molecular genetic heterogeneity in supratentorial and infratentorial primitive neuroectodermal tumors of the central nervous system. Cancer Genet Cytogenet. 1997; 97:25–31. [PubMed: 9242214]
7. Tabori U, Baskin B, Shago M, Alon N, Taylor MD, Ray PN, et al. Universal poor survival in children with medulloblastoma harboring somatic TP53 mutations. J Clin Oncol. 2010; 28:1345–1350. [PubMed: 20142599]
8. Frank AJ, Hernan R, Hollander A, Lindsey JC, Lusher ME, Fuller CE, et al. The TP53-ARF tumor suppressor pathway is frequently disrupted in large/cell anaplastic medulloblastoma. Brain research Molecular brain research. 2004; 121:137–140. [PubMed: 14969745]
9. Northcott PA, Shih DJ, Peacock J, Garzia L, Morrissy AS, Zichner T, et al. Subgroup-specific structural variation across 1,000 medulloblastoma genomes. Nature. 2012; 488:49–56. [PubMed: 22832581]
10. Oliver TG, Read TA, Kessler JD, Mehmeti A, Wells JF, Huynh TT, et al. Loss of patched and disruption of granule cell development in a pre-neoplastic stage of medulloblastoma. Development. 2005; 132:2425–2439. [PubMed: 15843415]
11. Schuller U, Heine VM, Mao J, Kho AT, Dillon AK, Han YG, et al. Acquisition of granule neuron precursor identity is a critical determinant of progenitor cell competence to form Shh-induced medulloblastoma. Cancer Cell. 2008; 14:123–134. [PubMed: 18691547]
12. Marino S, Vooijs M, van Der Gulden H, Jonkers J, Berns A. Induction of medulloblastomas in p53-null mutant mice by somatic inactivation of Rb in the external granular layer cells of the cerebellum. Genes Dev. 2000; 14:994–1004. [PubMed: 10783170]
13. Wechsler-Reya RJ, Scott MP. Control of neuronal precursor proliferation in the cerebellum by Sonic Hedgehog. Neuron. 1999; 22:103–114. [PubMed: 10027293]
14. Doucette TA, Yang Y, Pedone C, Kim JY, Dubuc A, Northcott PD, et al. WIP1 enhances tumor formation in a sonic hedgehog-dependent model of medulloblastoma. Neurosurgery. 2012; 70:1003–1010. discussion 1010. [PubMed: 22037313]
15. Pandolfi S, Montagnani V, Penachioni JY, Vinci MC, Olivito B, Borgognoni L, et al. WIP1 phosphatase modulates the Hedgehog signaling by enhancing GLI1 function. Oncogene. 2012
16. Hyman JM, Firestone AJ, Heine VM, Zhao Y, Ocasio CA, Han K, et al. Small-molecule inhibitors reveal multiple strategies for Hedgehog pathway blockade. Proc Natl Acad Sci U S A. 2009; 106:14132–14137. [PubMed: 19666565]

17. Chen JK, Taipale J, Young KE, Maiti T, Beachy PA. Small molecule modulation of Smoothened activity. Proc Natl Acad Sci U S A. 2002; 99:14071–14076. [PubMed: 12391318]
18. Vassilev LT, Vu BT, Graves B, Carvajal D, Podlaski F, Filipovic Z, et al. In vivo activation of the p53 pathway by small-molecule antagonists of MDM2. Science. 2004; 303:844–848. [PubMed: 14704432]
19. Hallahan AR, Pritchard JI, Hansen S, Benson M, Stoeck J, Hatton BA, et al. The SmoA1 mouse model reveals that notch signaling is critical for the growth and survival of sonic hedgehog-induced medulloblastomas. Cancer Res. 2004; 64:7794–7800. [PubMed: 15520185]
20. Bhatia B, Malik A, Fernandez LA, Kenney AM. p27(Kip1), a double-edged sword in Shh-mediated medulloblastoma: Tumor accelerator and suppressor. Cell Cycle. 2010; 9:4307–4314. [PubMed: 21051932]
21. Demidov ON, Kek C, Shreeram S, Timofeev O, Fornace AJ, Appella E, et al. The role of the MKK6/p38 MAPK pathway in Wip1-dependent regulation of ErbB2-driven mammary gland tumorigenesis. Oncogene. 2007; 26:2502–2506. [PubMed: 17016428]
22. Nannenga B, Lu X, Dumble M, Van Maanen M, Nguyen TA, Sutton R, et al. Augmented cancer resistance and DNA damage response phenotypes in PPM1D null mice. Mol Carcinog. 2006; 45:594–604. [PubMed: 16652371]
23. Bulavin DV, Phillips C, Nannenga B, Timofeev O, Donehower LA, Anderson CW, et al. Inactivation of the Wip1 phosphatase inhibits mammary tumorigenesis through p38 MAPK-mediated activation of the p16(Ink4a)-p19(Arf) pathway. Nat Genet. 2004; 36:343–350. [PubMed: 14991053]
24. Rodon J, Tawbi HA, Thomas AL, Stoller RG, Turtschi CP, Baselga J, et al. A phase I, multicenter, open-label, first-in-human, dose-escalation study of the oral smoothened inhibitor Sonidegib (LDE225) in patients with advanced solid tumors. Clin Cancer Res. 2014; 20:1900–1909. [PubMed: 24523439]
25. Emelyanov A, Bulavin DV. Wip1 phosphatase in breast cancer. Oncogene. 2014
26. Bulavin DV, Demidov ON, Saito S, Kauraniemi P, Phillips C, Amundson SA, et al. Amplification of PPM1D in human tumors abrogates p53 tumor-suppressor activity. Nat Genet. 2002; 31:210–215. [PubMed: 12021785]
27. Saito-Ohara F, Imoto I, Inoue J, Hosoi H, Nakagawara A, Sugimoto T, et al. PPM1D is a potential target for 17q gain in neuroblastoma. Cancer Res. 2003; 63:1876–1883. [PubMed: 12702577]
28. Castellino RC, De Bortoli M, Lu X, Moon SH, Nguyen TA, Shepard MA, et al. Medulloblastomas overexpress the p53-inactivating oncogene WIP1/PPM1D. J Neurooncol. 2008; 86:245–256. [PubMed: 17932621]
29. Buss MC, Read TA, Schniederjan MJ, Gandhi K, Castellino RC. HDM2 promotes WIP1-mediated medulloblastoma growth. Neuro Oncol. 2012; 14:440–458. [PubMed: 22379189]
30. Ellison DW, Dalton J, Kocak M, Nicholson SL, Fraga C, Neale G, et al. Medulloblastoma: clinicopathological correlates of SHH, WNT, and non-SHH/WNT molecular subgroups. Acta Neuropathol. 2011; 121:381–396. [PubMed: 21267586]
31. Buss MC, Remke M, Lee J, Gandhi K, Schniederjan MJ, Kool M, et al. The WIP1 oncogene promotes progression and invasion of aggressive medulloblastoma variants. Oncogene. 2015; 34:1126–1140. [PubMed: 24632620]
32. Lu X, Nguyen TA, Zhang X, Donehower LA. The Wip1 phosphatase and Mdm2: cracking the “Wip” on p53 stability. Cell Cycle. 2008; 7:164–168. [PubMed: 18333294]
33. Stecca B, Ruiz i Altaba A. A GLI1-p53 inhibitory loop controls neural stem cell and tumour cell numbers. Embo J. 2009; 28:663–676. [PubMed: 19214186]
34. Abe Y, Oda-Sato E, Tobiume K, Kawauchi K, Taya Y, Okamoto K, et al. Hedgehog signaling overrides p53-mediated tumor suppression by activating Mdm2. Proc Natl Acad Sci U S A. 2008; 105:4838–4843. [PubMed: 18359851]
35. Doucette TA, Yang Y, Pedone C, Kim JY, Dubuc A, Northcott PD, et al. WIP1 Enhances Tumor Formation in a Sonic Hedgehog-Dependent Model of Medulloblastoma. Neurosurgery. 2012
36. Rayter S, Elliott R, Travers J, Rowlands MG, Richardson TB, Boxall K, et al. A chemical inhibitor of PPM1D that selectively kills cells overexpressing PPM1D. Oncogene. 2008; 27:1036–1044. [PubMed: 17700519]

37. Gilmartin AG, Faitg TH, Richter M, Groy A, Seefeld MA, Darcy MG, et al. Allosteric Wip1 phosphatase inhibition through flap-subdomain interaction. Nature chemical biology. 2014; 10:181–187. [PubMed: 24390428]

38. Yoda A, Toyoshima K, Watanabe Y, Onishi N, Hazaka Y, Tsukuda Y, et al. Arsenic trioxide augments Chk2/p53-mediated apoptosis by inhibiting oncogenic Wip1 phosphatase. J Biol Chem. 2008; 283:18969–18979. [PubMed: 18482988]

39. Parathath SR, Mainwaring LA, Fernandez LA, Campbell DO, Kenney AM. Insulin receptor substrate 1 is an effector of sonic hedgehog mitogenic signaling in cerebellar neural precursors. Development. 2008; 135:3291–3300. [PubMed: 18755774]

40. Castellino RC, De Bortoli M, Lin LL, Skapura DG, Rajan JA, Adesina AM, et al. Overexpressed TP73 induces apoptosis in medulloblastoma. BMC Cancer. 2007; 7:127. [PubMed: 17626635]

41. Lamprecht MR, Sabatini DM, Carpenter AE. CellProfiler: free, versatile software for automated biological image analysis. Biotechniques. 2007; 42:71–75. [PubMed: 17269487]

42. Choi J, Nannenga B, Demidov ON, Bulavin DV, Cooney A, Brayton C, et al. Mice deficient for the wild-type p53-induced phosphatase gene (Wip1) exhibit defects in reproductive organs, immune function, and cell cycle control. Mol Cell Biol. 2002; 22:1094–1105. [PubMed: 11809801]

43. Yang ZJ, Ellis T, Markant SL, Read TA, Kessler JD, Bourboulas M, et al. Medulloblastoma can be initiated by deletion of Patched in lineage-restricted progenitors or stem cells. Cancer Cell. 2008; 14:135–145. [PubMed: 18691548]

44. Kenney AM, Cole MD, Rowitch DH. Nmyc upregulation by sonic hedgehog signaling promotes proliferation in developing cerebellar granule neuron precursors. Development. 2003; 130:15–28. [PubMed: 12441288]

45. Suresh K. An overview of randomization techniques: An unbiased assessment of outcome in clinical research. J Hum Reprod Sci. 2011; 4:8–11. [PubMed: 21772732]

46. Hatton BA, Villavicencio EH, Tsuchiya KD, Pritchard JI, Ditzler S, Pullar B, et al. The Smo/Smo model: hedgehog-induced medulloblastoma with 90% incidence and leptomeningeal spread. Cancer research. 2008; 68:1768–1776. [PubMed: 18339857]

47. Vanner RJ, Remke M, Gallo M, Selvadurai HJ, Coutinho F, Lee L, et al. Quiescent sox2(+) cells drive hierarchical growth and relapse in sonic hedgehog subgroup medulloblastoma. Cancer Cell. 2014; 26:33–47. [PubMed: 24954133]

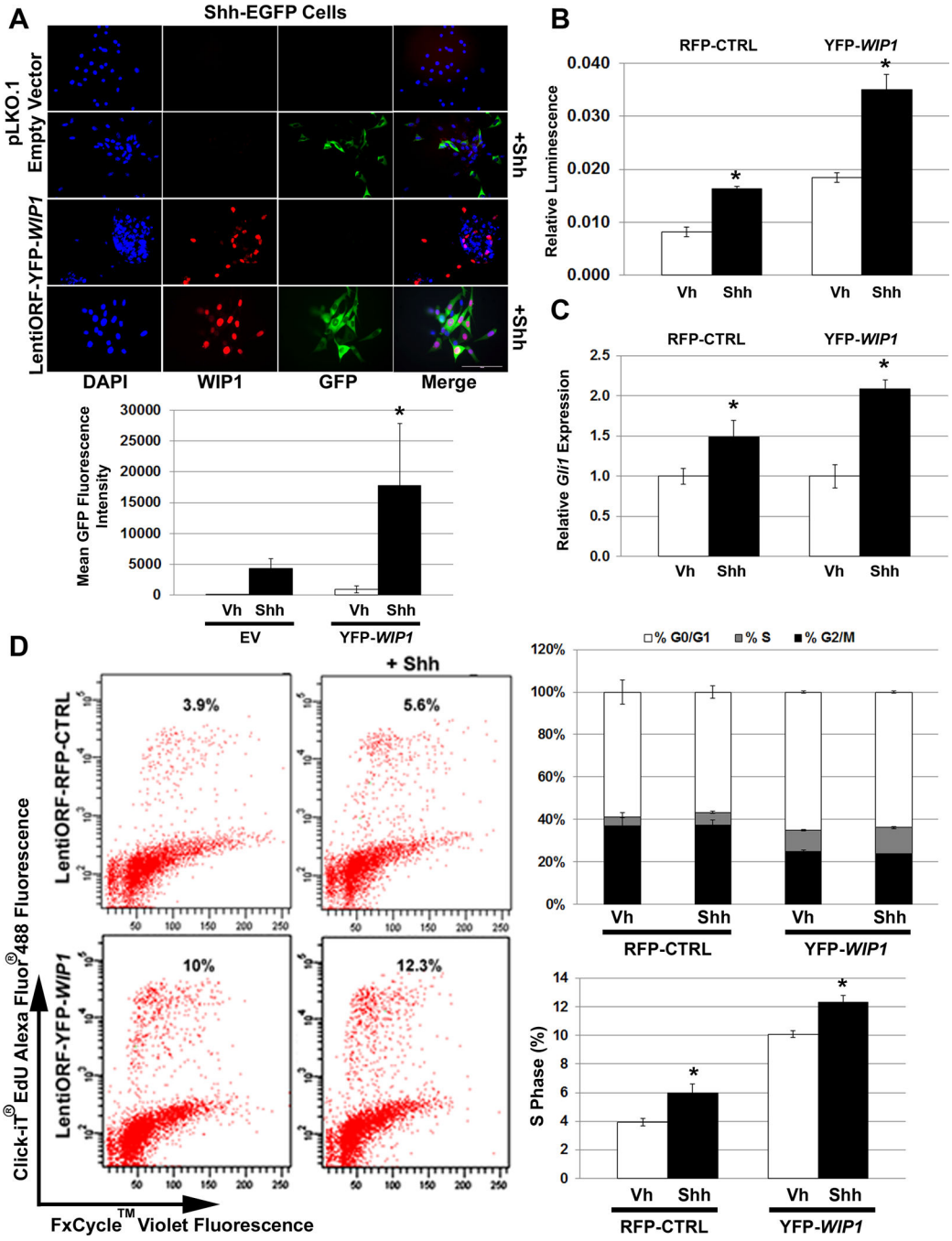

Figure 1. *WIP1* promotes cell growth through hedgehog pathways

(**A**) Twenty-four hours after 1×10^5 Shh-EGFP cells were seeded on poly-L ornithine-coated plates, cells were transduced with empty vector (pLKO.1) or yellow (YFP) fluorescent protein-tagged *WIP1* (YFP-*WIP1*) lentivirus and stimulated with vehicle (Vh) or Shh (Shh-N recombinant protein, 3μg/mL) for another 24 hours, followed by fixation and incubation with α-WIP1 primary and RFP-tagged secondary antibodies. Representative photomicrographs show fluorescence for DAPI, RFP, and GFP (top panel). Total fluorescence was measured using CellProfiler software (bottom panel), *p<0.0001. Scale

bar, 100μm. (**B**) Shh-LIGHT2 cells were transduced with control red (RFP) fluorescent protein-tagged (RFP-CTRL) or YFP-*WIP1* lentivirus and stimulated with Vh or Shh for 24 hours. Cells were subsequently lysed and assayed for expression of Firefly luciferase, relative to Renilla luciferase, *$p<0.005$. (**C**) Shh-EGFP cells, transduced with RFP-CTRL or YFP-*WIP1* lentivirus and stimulated with Vh or Shh for 24 hours, were harvested and lysed for total RNA. mRNA was used to determine expression of *Gli1*, relative to *Gapdh* and normalized to expression in Vh-treated cells, by real-time, RT-PCR, *$p<0.005$. (**D**) Shh-EGFP cells were treated as in (**C**), then incubated with 10μM Click-iT EdU for 2 hours, followed by detection of cell cycle by flow cytometry. Error bars, standard deviation (SD) among replicates of at least three per treatment. All experiments were repeated at least three times.

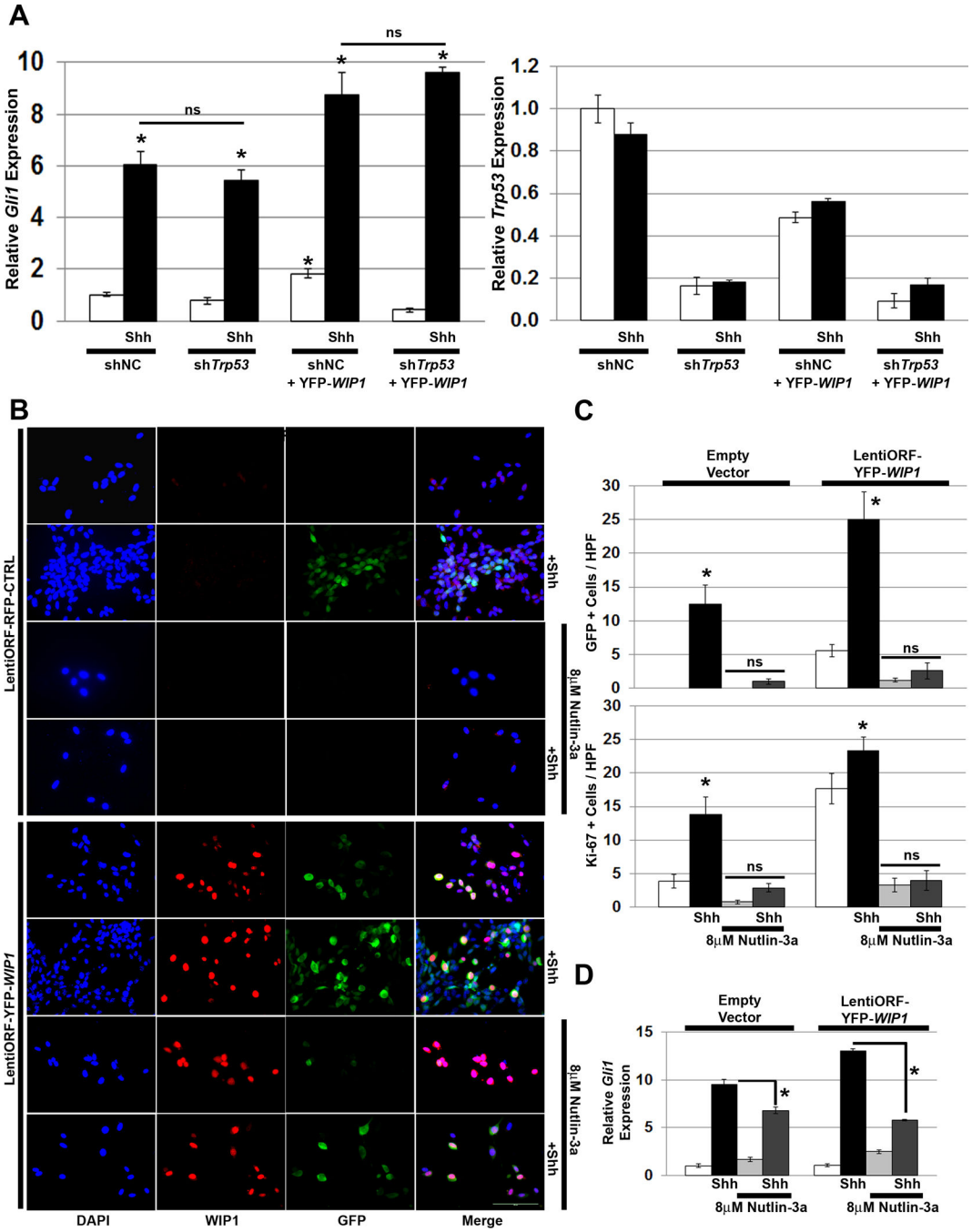

Figure 2. *WIP1* enhances hedgehog signaling independent of p53

(**A**) Twenty-four hours after plating 1×10^5 Shh-EGFP cells, media was changed to serum-free media containing vehicle or Shh (3μg/mL). Cells were transduced with lentivirus containing negative control (shNC) or *Trp53* shRNA (sh*Trp53*) in combination with lentivirus containing an empty vector or YFP-tagged *WIP1* cDNA (LentiORF-YFP-*WIP1*), and incubated for another 48 hours. Shown is real-time, RT-PCR for *Gli1* and *Trp53*, relative to *Gapdh* and normalized to vehicle-treated, shNC and empty vector-transduced controls, *$p<0.005$. (**B**) Twenty-four hours after plating 1×10^5 Shh-EGFP cells, media was changed to

serum-free media containing vehicle, 8μM Nutlin-3a, and/or Shh (3μg/mL). Cells were also transduced with lentivirus containing pLKO.1 empty vector or LentiORF-YFP-*WIP1*. 48 hours later, cells were fixed in 4% paraformaldehyde, permeabilized, incubated with α-WIP1 or α-Ki-67 antibody, and mounted using media containing DAPI. Scale bar, 100μm. (**C**) Quantitation of cells from (**B**) that express green fluorescent protein (GFP) or Ki-67, per high power field (HPF). Bars, mean cell counts from 10 representative fields for each condition, *p<0.005. (**D**) mRNA was used to determine *Gli1*, relative to *Gapdh* and normalized to expression in empty vector-transduced, vehicle-treated cells, by real-time, RT-PCR, *p<0.005. Error bars, standard deviation (SD) among replicates of at least three per treatment. All experiments were repeated at least three times. ns, not significant.

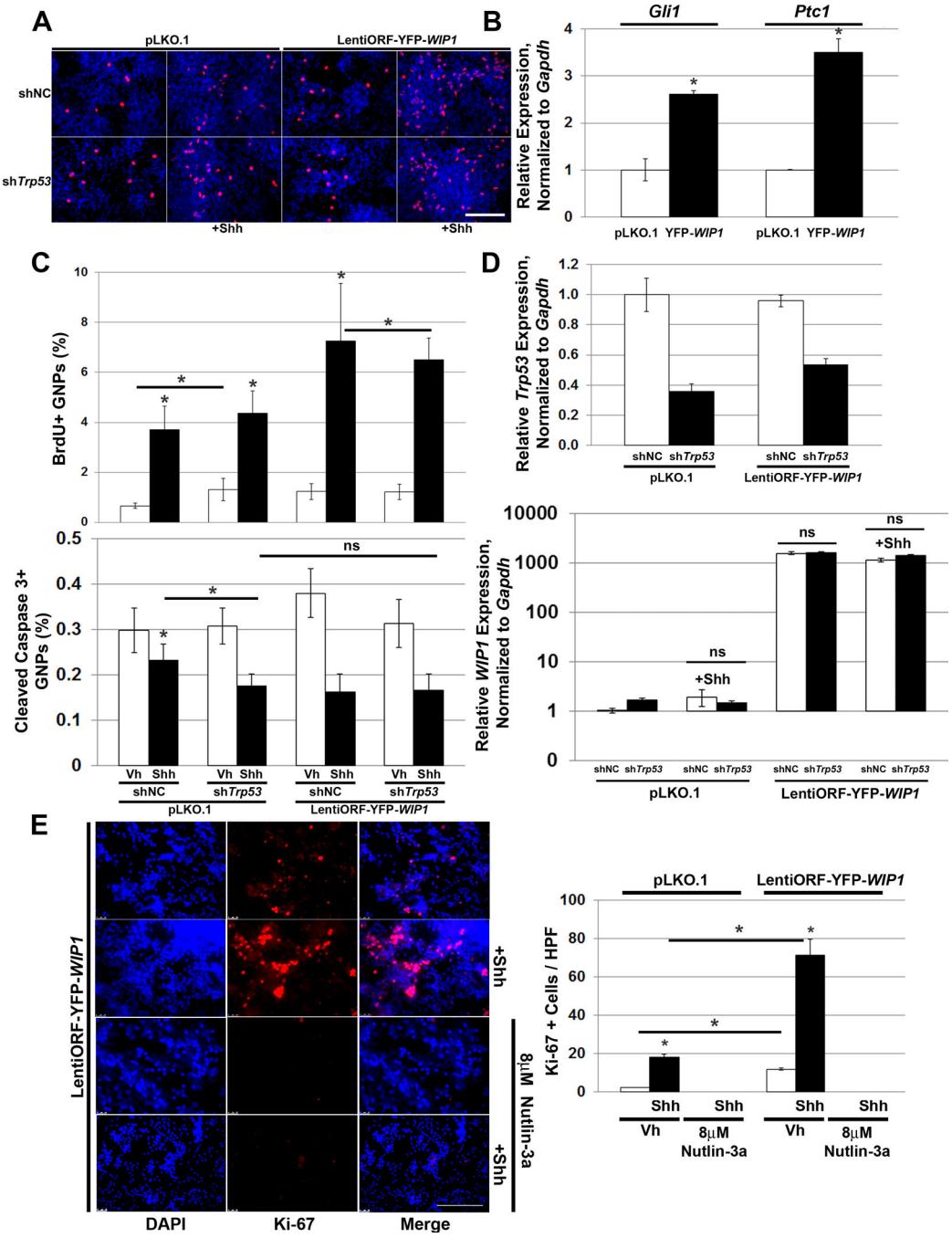

Figure 3. *WIP1* enhances hedgehog signaling and proliferation of cerebellar granule neuron precursor cells

(**A**) Three hours after plating 1×10^6 post-natal day five (P5) cerebellar granule neuron precursor cells (GNPs), media was changed to serum-free media containing vehicle or Shh (3μg/mL) and cells were transduced with lentivirus containing shNC or sh*Trp53* in combination with lentivirus containing empty vector or LentiORF-YFP-*WIP1*. 48 hours later, cells were incubated with 3μg/mL BrdU for four hours, fixed in 4% paraformaldehyde (PFA), permeabilized, and incubated with α-BrdU antibody, followed by Alexa Fluor 594-

conjugated secondary antibody. Shown are representative photomicrographs 48 hours after viral transduction. BrdU, red; DAPI, blue. Scale bar, 100μm. (**B**) Lentivirus-transduced GNPs from (**A**) were examined by real-time, RT-PCR for *Gli1* and *Ptc1*, relative to *Gapdh* and normalized to empty vector-transduced controls, *p<0.005. (**C**) Quantitation of GNPs, from (**A**), that fluoresce positive for BrdU (top panel) or Cleaved Caspase 3 (bottom panel), relative to DAPI, using CellProfiler software, *p<0.005. (**D**) Real-time, RT-PCR for *Trp53* (top panel) or *WIP1* (bottom panel), relative to *Gapdh* and normalized to vehicle-treated, shNC-transduced controls, *p<0.005. (**E**) Twenty-four hours after plating 1×10^6 P5 GNPs, media was changed to serum-free media containing vehicle, 8μM Nutlin-3a, and/or Shh (3μg/mL). Cells were also transduced with lentivirus containing pLKO.1 or LentiORF-YFP-*WIP1*. 48 hours later, cells were fixed in 4% PFA, permeabilized, incubated with α-Ki-67 antibody, and mounted using media containing DAPI (left-hand panel). Scale bar, 100μm. Quantitation of cells from (**C**) that express Ki-67, per high power field (HPF) (right-hand panel), *p<0.005. Bars, mean of cell counts from 10 representative fields for each experimental condition. Error bars, standard deviation (SD) among replicates of at least three per treatment. All experiments were repeated at least three times.

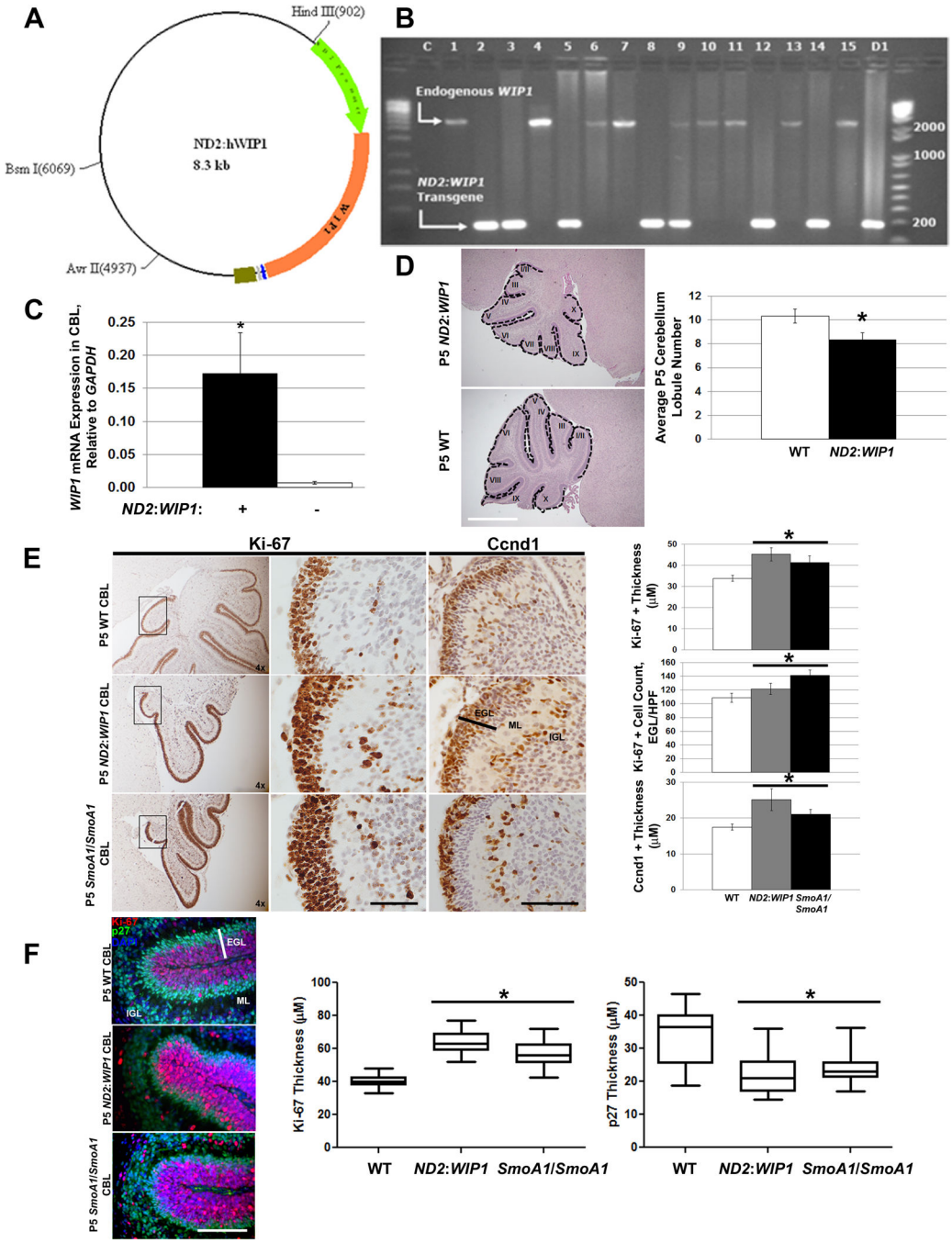

Figure 4. *WIP1* promotes increased proliferation and downstream hedgehog signaling in the neonatal cerebellum

(**A**) Schematic of construct used to generate *ND2*: *WIP1* transgenic mice, showing a 1-kb portion of the *Neurod2* (*ND2*) promoter (green arrow) driving expression of *WIP1* (orange arrow; 1.8-kb). (**B**) DNA gel showing RT-PCR results from tail snips of *ND2*: *WIP1* transgenic founder mice using primers spanning exons 4 and 5 of *WIP1*: expected 2485 base pair (bp) PCR product from endogenous *Wip1*; 180bp PCR product from *WIP1* cDNA from expression construct in (**A**). C, empty template control; 1–15, founder mice; D1, PCR

product using *ND2*: *WIP1* construct as template. DNA ladders shown on either side of gel, with notations for 200–2000bp. (**C**) *WIP1* expression by real-time RT-PCR in the cerebellum of P7 *ND2*: *WIP1* transgenic, relative to *Gapdh*, compared to expression in the cerebellum of P7 wild-type (WT) C57Bl/6 mice, *$p<0.005$. (**D**) Hematoxylin and eosin stained P5 cerebella of WT and *ND2*: *WIP1* transgenic mice (left-hand panel). Dotted line, cerebellar lobules (I–X). Quantitation of cerebellar lobules in P5 WT and *ND2*: *WIP1* transgenic mice (right-hand panel) (n=3 cerebella per genotype), *$p<0.05$. (**E**) Immunohistochemical staining (left-hand panels) and quantitation (right-hand panels) of Ki-67 and the downstream marker of hedgehog pathway activation, Cyclin D1 (Ccnd1), in the external granule layer (EGL) of lobule X of the cerebellum of P5 wild-type, *ND2*: *WIP1*, and *SmoA1*/*SmoA1* mice, *$p<0.05$. Bar, EGL width. (**F**) Immunofluorescent staining (left-hand panels) and quantitation (right-hand panels) of Ki-67 and $p27^{Kip1}$ (p27), in the external granule layer (EGL) of the cerebellum of P5 wild-type, *ND2*: *WIP1*, and *SmoA1*/*SmoA1* mice (n=3 cerebella per genotype), *$p<0.005$. Ki67, red; p27, green; DAPI, blue. Bar, EGL width. ML, molecular layer; IGL, internal granule layer; HPF, high-power field. Error bars, standard deviation (SD) among replicates of at least three per group. Scale bars, 100μm. All experiments were repeated at least three times or in at least three distinct cerebella.

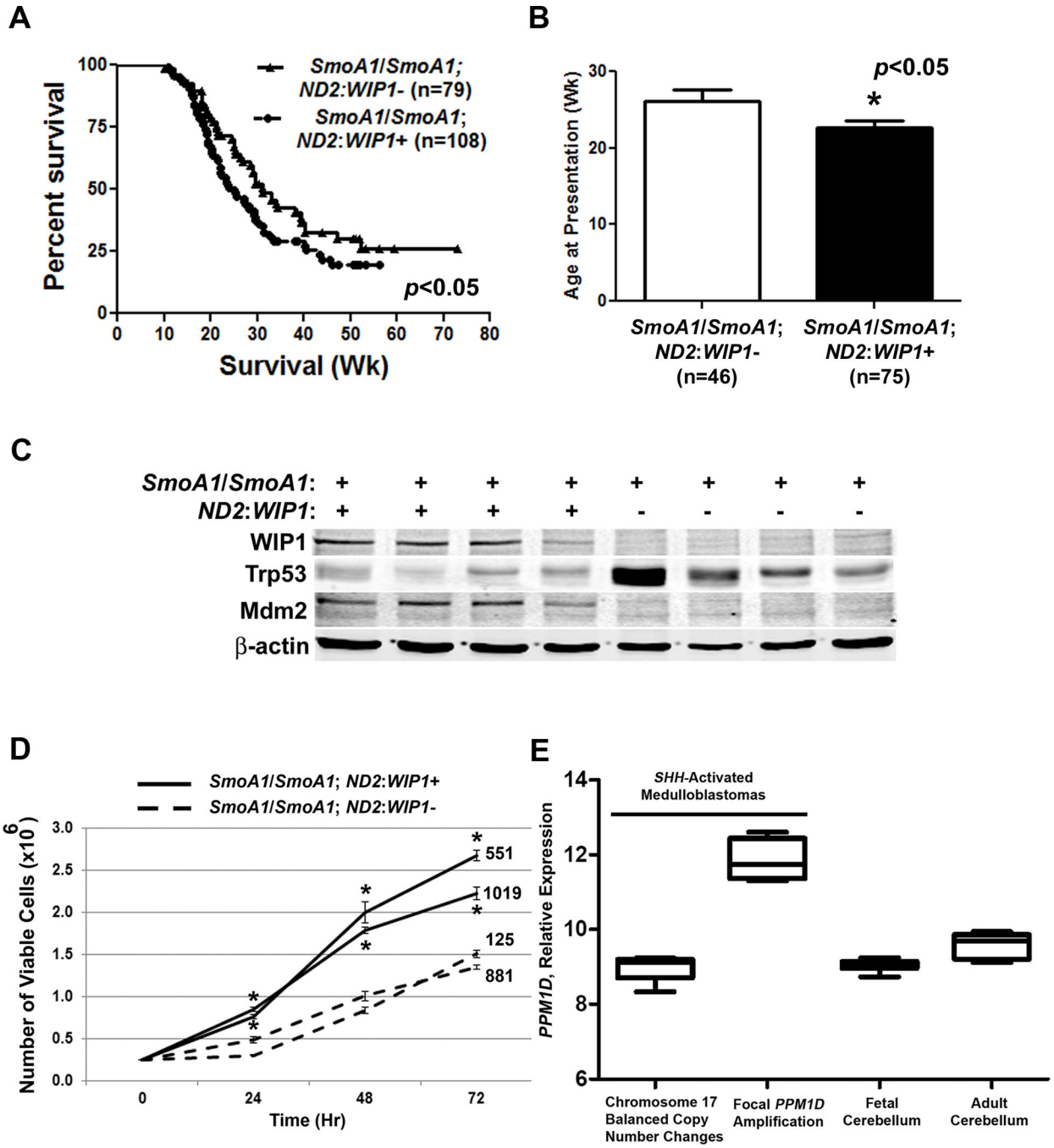

Figure 5. *WIP1* promotes increased tumor incidence and reduced survival in a hedgehog-activated MB model

(**A**) Kaplan-Meier curves showing overall, MB-related survival of *SmoA1*/*SmoA1*; *ND2*: *WIP1*-(*WIP1* transgene absent by RT-PCR) versus *SmoA1*/*SmoA1*; *ND2*: *WIP1*+ (*WIP1* transgene present) mice, **p*<0.05. n, mice per group. (**B**) Age of mice at time of presentation with symptoms of medulloblastoma (MB), **p*<0.05. (**C**) Representative western blots for WIP1, Trp53, and Mdm2 from lysates of MBs harvested from symptomatic *SmoA1*/*SmoA1*; *ND2*: *WIP1*- and *SmoA1*/*SmoA1*; *ND2*: *WIP1*+ mice. β-actin, loading control. (**D**) 2.5×10^5

MB cells from symptomatic mice were plated in triplicate in serum-containing media and assayed for viability by trypan blue exclusion, *$p<0.05$. (**E**) Relative *WIP1* expression in human MBs with balanced copy number changes of chromosome 17 (n=5) or focal amplification of the *WIP1* gene locus (n=4) by Affymetrix SNPs. Both MB groups exhibit a gene signature consistent with activation of hedgehog signaling. Shown for comparison is *WIP1* expression in human fetal and adult cerebellum (n=6, each). Error bars, standard deviation (SD) among replicates of at least three per group. All experiments were repeated at least three times.

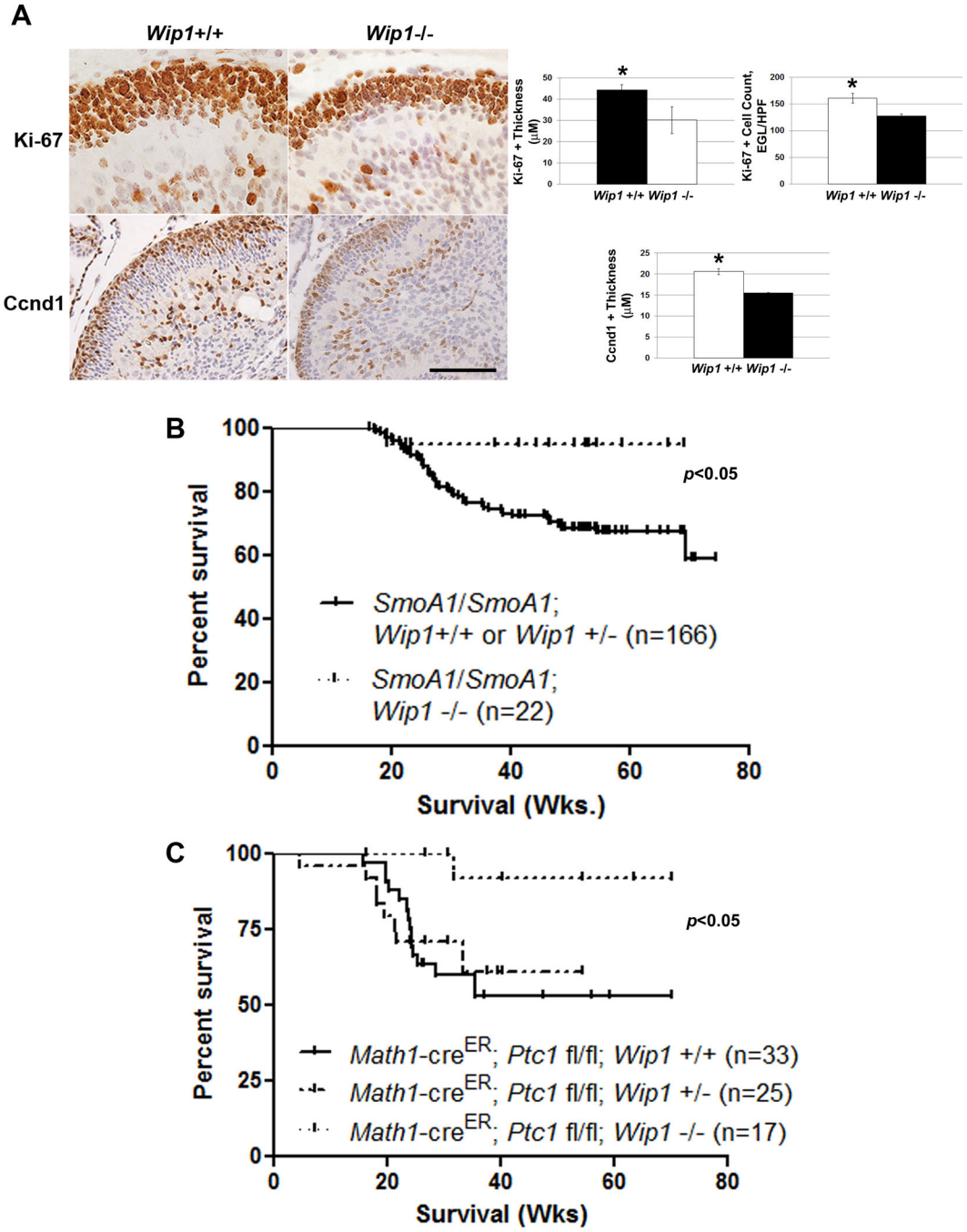

Figure 6. *Wip1* knock-out suppresses MB formation in hedgehog-activated MB models

(**A**) Immunohistochemical staining (left-hand panels) and quantitation (right-hand panels) of Ki-67+ and Cyclin D1 (Ccnd1)+ cells in the external granule layer of the cerebellum of P5 *Wip1*+/+ and *Wip1*−/− mice (n=3 cerebella per genotype), **p*<0.005. Scale bar, 100μm. (**B**) Kaplan-Meier curves showing overall, MB-related survival of *SmoA1*/*SmoA1*; *Wip1*+/+, *SmoA1*/*SmoA1*; *Wip1*+/−, and *SmoA1*/*SmoA1*; *Wip1*−/− mice. (**C**) Kaplan-Meier curves showing overall, MB-related survival of *Math1*-cre^{ER}; *Ptc1* fl/fl; *Wip1*+/+, *Math1*-cre^{ER};

Ptc1 fl/fl; *Wip1*+/−, and *Math1*-cre^{ER}; *Ptc1* fl/fl; *Wip1*−/− mice following treatment with 1mg tamoxifen by oral gavage per mouse at P7.

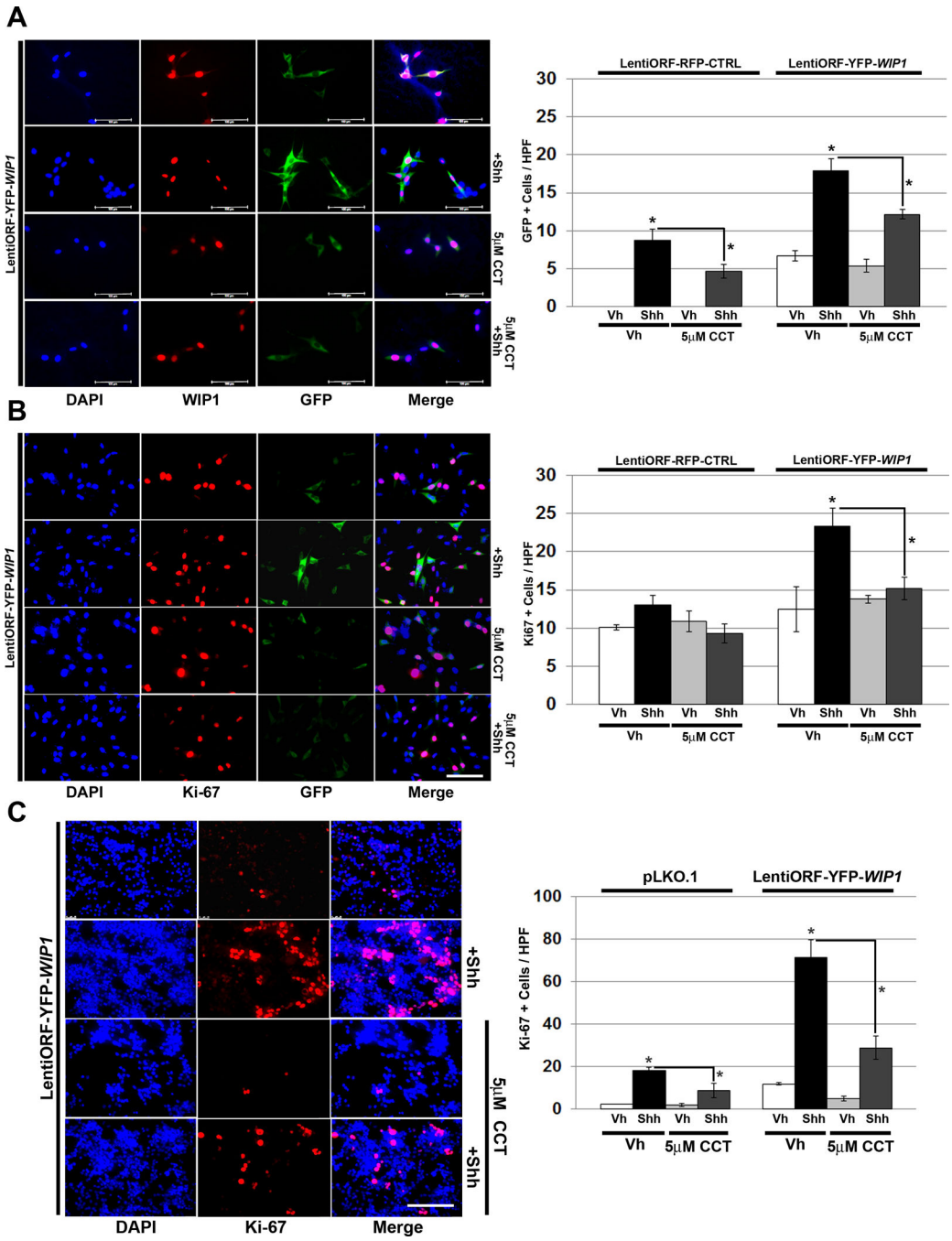

Figure 7. WIP1 inhibition suppresses hedgehog-mediated cell growth

(**A–B**)Twenty-four hours after plating 1×10^5 shh-EGFP cells, media was changed to serum-free media containing vehicle (Vh), DMSO, CCT007093 (CCT, 5μM), and/or Shh (3μg/mL). Cells were also transduced with LentiORF-RFP-CTRL or LentiORF-YFP-*WIP1* lentivirus. 48 hours later, cells were fixed in 4% paraformaldehyde, permeabilized, incubated with α-WIP1 or α-Ki-67 antibody, and mounted using media containing DAPI (left-hand panels). Quantification of cells, per high power field (HPF), that express green fluorescent protein (GFP) or Ki-67 (right-hand panels). Bars, mean of cell counts from 10 representative fields

for each experimental condition. (**C**) Twenty-four hours after plating 1×10^6 P5 GNPs, media was changed to serum-free media containing vehicle, 5μM CCT, and/or Shh (3μg/mL). Cells were also transduced with lentivirus containing pLKO.1 or LentiORF-YFP-*WIP1*. 48 hours later, cells were fixed in 4% paraformaldehyde, permeabilized, incubated with α-Ki-67 antibody, and mounted using media containing DAPI (left-hand panel). Quantification of cells from (**C**), per high power field (HPF), that express Ki-67 (right-hand panel). Error bars, standard deviation (SD) among replicates of at least three per treatment. Scale bars, 100μm. All experiments were repeated at least three times. *$p<0.005$.

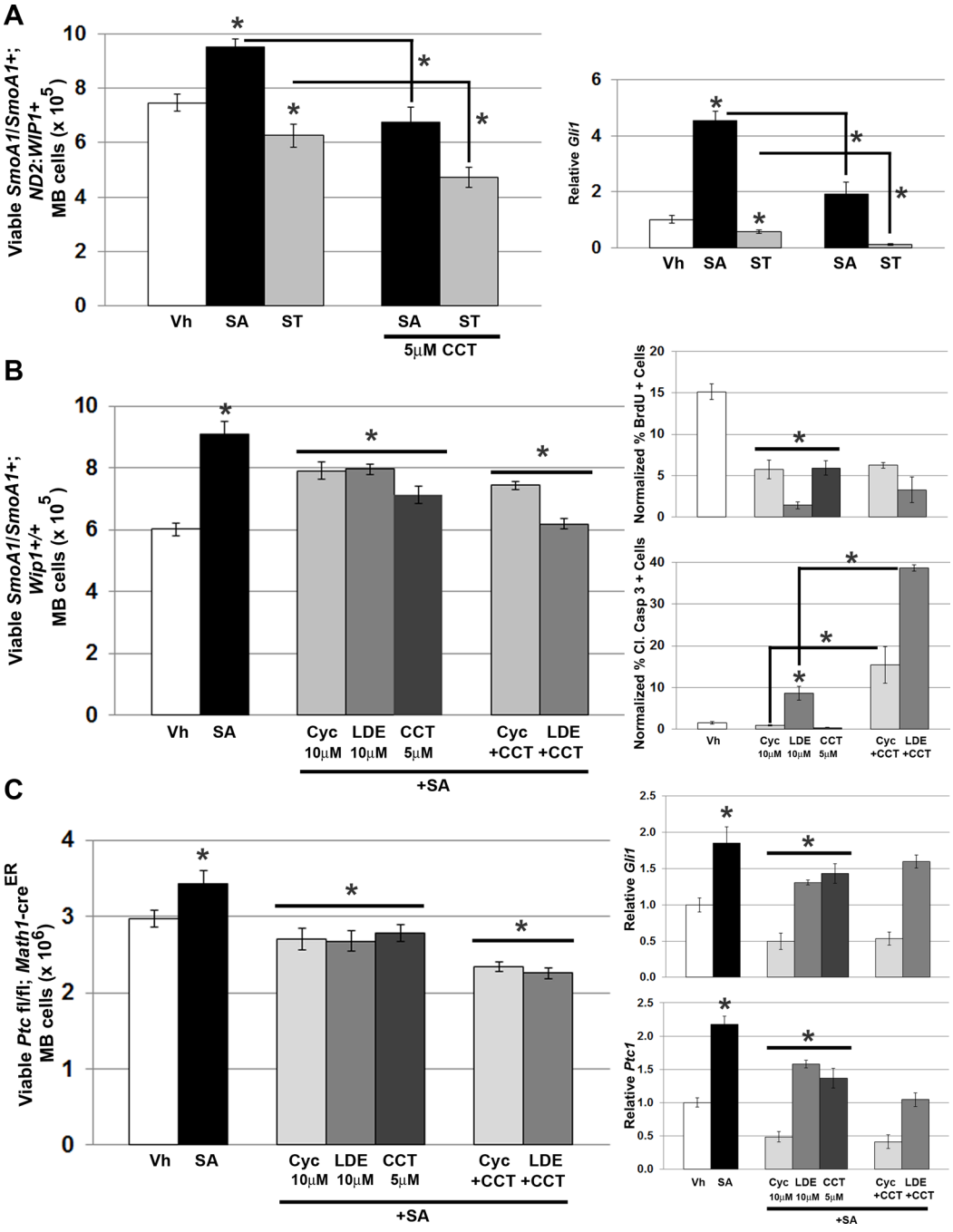

Figure 8. WIP1 inhibition augments inhibition of hedgehog signaling in hedgehog-activated MB cells

(**A**). Twenty-four hours after plating 1×10^6 MB cells from symptomatic *SmoA1*/*SmoA1*; *ND2*: *WIP1*+ mice, media was changed to serum-free media containing vehicle (Vh), DMSO, 200nM SAG, or 100nM SANT-1, with or without CCT007093 (5μM, CCT). Viable cells were determined by trypan blue exclusion (left-hand panel), *$p<0.05$. Real-time, RT-PCR for *Gli1*, relative to *Gapdh* and normalized to vehicle-treated controls, using cells from (**A**) (right-hand panel), *$p<0.05$. (**B**) Twenty-four hours after plating 1×10^6 MB cells derived

from symptomatic *SmoA1*/*SmoA1*; *Wip1+/+* or (**C**) tamoxifen-induced *Math1*-cre^{ER}; *Ptc1* fl/fl mice (left-hand panels), media was changed to serum-free media containing vehicle (Vh), 200nM SAG, 10μM cyclopamine (Cyc), 10μM LDE225 (LDE), or 5μM CCT, with or without Cyc or LDE. Cells were incubated under tissue culture conditions for another 24 hours. Viable cells were determined by trypan blue exclusion (left-hand panel), *p<0.05. Real-time, RT-PCR for *Gli1*and *Ptc1*, relative to *Gapdh* and normalized to vehicle-treated controls, in cells from (**C**) (right-hand panels), *p<0.05. Medulloblastoma cells from symptomatic *SmoA1*/*SmoA1*; *Wip1+/+* were also treated with Vh, 10μM Cyc, 10μM LDE, or 5μM CCT, with or without Cyc or LDE, followed by incubation with 3μg/mL BrdU for four hours, fixation in 4% PFA, permeabilization, and incubation with α-BrdU antibody, followed by incubation with Alexa Fluor 594-conjugated secondary antibody. Shown is quantitation of BrdU (**B**, top-right panel) or Cleaved Caspase 3 (**B**, bottom-right panel) immunofluorescence, relative to DAPI using CellProfiler software, *p<0.005. Error bars, standard deviation (SD) among replicates of at least three per treatment. All experiments were repeated at least three times.